Twenty-Sixth Symposium (International) on Combustion/The Combustion Institute, 1996/pp. 1523–1530

NUMERICAL SIMULATION OF COMBUSTION IN FIRE PLUMES

WILLIAM E. MELL, KEVIN B. MCGRATTAN AND HOWARD R. BAUM
National Institute of Standards and Technology
Gaithersburg, Maryland 20899-0001, USA

Combustion in buoyancy-driven fire plumes is assumed to be diffusion controlled and described by a mixture fraction variable. Experimental data for a 10-cm methanol pool fire was compared to numerical results obtained by assuming the plume was axially symmetric. No turbulence model was used. The influence of imposing axial symmetry independent of the approximations made in the combustion model was tested by comparing simulated and experimental helium plumes. Simulated helium plume results agreed well with the experimental data at sufficiently small heights where most combustion occurs. At larger heights, predictions from the helium simulations were increasingly in error within a volume surrounding the centerline. Prediction error in the pool fire simulations behaved largely in a similar manner, with some error present due to inadequacies in the mixture-fraction-based combustion model. Overall, within the limitations of an axially-symmetric calculation, the behavior of flame flickering and the time-averaged temperature field were reasonably well predicted.

Introduction

One of the central issues in fire research is the structure of an isolated fire plume. Numerical modeling of a fire plume is difficult for two fundamental reasons. First, in a typical laboratory experiment, combustion occurs at the base of the plume in a region that occupies a small fraction (1–2%) of the overall volume containing the plume and the surrounding source of entrained air. A numerical simulation of a small (10–20 cm diameter) pool fire, therefore, requires resolution of phenomena on length scales covering nearly three orders of magnitude: the reaction zone ($\approx$1 mm) to several pool diameters. Thus, even with a simple combustion model, it is not possible to directly solve the appropriate conservation equations for three-dimensional fire plumes using present-day computers. Second, the location of the combustion zone at the base of the plume varies due to the quasi-periodic formation of large-scale, low frequency toroidal vortices [1–2]. The plume dynamics are therefore inherently time dependent, even at the largest scales, making time-averaging model approaches (e.g., $k - \varepsilon$ turbulence model) inappropriate. Clearly, some idealization of the physical phenomena is required.

In the present work, the combustion in a pool fire was idealized to be diffusion controlled, permitting a mixture-fraction-based modeling approach. The major physical limitations of the approach are that it idealizes radiative heat transfer and does not account for finite rate reaction, nonunity Lewis number, or multistep chemistry effects. While these effects are of varying importance, they can not all be included due to computational cost. What was captured in the model is the chemical heat release which is the source of buoyancy and drives the flow. Thus, this combustion model is an appropriate first step to modeling fire-driven buoyant plumes. The hydrodynamics was simplified by assuming the plume was axially symmetric. With these approximations, molecular values of the transport coefficients could be used for plumes of sufficiently small scale (i.e., no closure models were used and these were direct numerical simulations in the axially-symmetric limit). The validity of assuming axial symmetry was tested by comparing simulated and experimental helium plumes. The combustion model was then used in the simulation of a 10-cm-diameter methanol pool fire experiment. Both time-averaged and time-resolved (in the form of video recordings) measurements were compared to the simulations. Differences between the simulated and experimental fire plume, not present in the helium plume, should be due largely to simplifications in the combustion model.

The governing equations were obtained by assuming the flow velocity is much smaller than the speed of sound [3] (low Mach number). The present approach is limited to the simulation of small fires. However, it can be readily adapted to more general scenarios when combined with a large eddy simulation approach which is based on approximating the source of buoyancy in a fire as a collection of small-scale thermal elements convected with the flow [4]. Indeed, a major goal of this work was to test the validity of the combustion model before applying it to the simulation of thermal elements. It is important to note that such a validity test is not possible if confounding effects from the use of a turbulence model are present.

Mixture-Fraction-Based Combustion Model

The combustion process is idealized as a single global reaction that proceeds at an effectively infinite rate whenever the reactants come into contact [5], as given by

$$\nu_F F + \nu_O O_2 \rightarrow \nu_C CO_2 + \nu_H H_2O \qquad (1)$$

where nitrogen is also present but chemically inactive. Here F denotes a hydrocarbon fuel molecule and ν_i the stoichiometric coefficient for species i. Let Y_i denote the mass fraction of species i. With the assumption of equal species mass diffusivities, $D_i = D$, the conservation equations for Y_F and Y_O can be combined to obtain the equation for the mixture fraction Z such that

$$\rho\left(\frac{\partial}{\partial t} + \underline{u}\cdot\nabla\right)Z = \nabla\cdot(\rho D\nabla Z) \qquad (2)$$

where

$$Z = \frac{Y_F/(\nu_F W_F) - Y_O/(\nu_O W_O) + Y_O^\infty/(\nu_O W_O)}{1/(\nu_F W_F) + Y_O^\infty/(\nu_O W_O)} \qquad (3)$$

Y_O^∞ is the value of Y_O in the ambient air, and W_i is the molecular weight of species i. An infinitely fast reaction results in $Y_F Y_O = 0$ with combustion taking place along an infinitesimally thin reaction sheet (in mixture fraction space) where $Y_F = Y_O = 0$ and Z equals its stoichiometric value $Z = Z_{st}$. The state relations for Y_F and Y_O, easily obtained from $Y_F Y_O = 0$ and equation 3, are piecewise linear functions of Z. Similarly, the state relations for Y_C, Y_H, and Y_N are also functions of Z.

Up to this point, only equal species diffusivities and fast chemistry have been assumed. It remains to determine the state relation for temperature and make further assumptions regarding thermal radiation. The classical approach (pp. 73–76 of Williams [6]) is to ignore thermal radiation, assume unit Lewis number, and deduce a piecewise linear relationship between the temperature and mixture fraction. However, thermal radiation is certainly not negligible in a fire plume. Moreover, there is experimental evidence [5] that the specific volume $v = 1/\rho$ is a better choice for a piecewise linear relationship with the mixture fraction. Given this assumption and the state relations for Y_i, the temperature can be determined from the equation of state for ideal gases

$$p_o = \mathcal{R}\rho T\sum_i \frac{Y_i}{W_i} \qquad (4)$$

Here, p_o is the spatially independent thermodynamic pressure [3], $\mathcal{R}$ is the universal gas constant, and T the temperature. With the relationship between specific volume and mixture fraction known from experimental studies [5], the complete combustion problem is governed by the conservation equations for the mixture fraction and momentum. Thermal radiation is accounted for in a global manner by assuming all locations in the flame have lost a fixed amount of chemical heat release through radiation to the surroundings [5].

To proceed, the empirically obtained normalized specific volume is fitted by the piecewise linear form

$$v(Z(\underline{x}, t)) = \frac{\rho_\infty(t)}{\rho} = \begin{cases} 1 + (v_{st} - 1)(Z/Z_{st}) \\ v_p + (v_{st} - v_p)(1 - Z)/(1 - Z_{st}) \end{cases}$$
$$0 \le Z \le Z_{st}$$
$$Z_{st} \le Z \le 1 \qquad (5)$$

where v_{st} and v_p are the normalized specific volume at the stoichiometric surface (flame surface) and pool (fuel surface), respectively, and ρ_∞ is the ambient air density. These density ratios can be related to their corresponding temperature ratios through the equation of state (equation 4). Note that ρ_∞ can vary with time when the domain is not open.

Equations of Motion

Following the analysis of Rehm and Baum [3], we assume that the flow velocity is much less than the sound speed; the temperature and density variations can be large, but the pressure variations are small. The gases are assumed to be ideal, specific heats are constant, and variable transport properties are used. The conservation equation for momentum is

$$\frac{\partial\rho\underline{u}}{\partial t} + \nabla\cdot(\rho\underline{u}\,\underline{u}) + \nabla p - (\rho - \rho_\infty)\underline{g} = \nabla\cdot\underline{\underline{\sigma}} \qquad (6)$$

Here, p is the perturbation pressure from ambient, $\underline{u}$ the velocity vector, $\underline{g}$ the acceleration of gravity, and $\underline{\underline{\sigma}}$ the standard viscosity stress tensor. Within the context of the present combustion model, the species equations have been replaced by the governing equation for the mixture fraction, equation 2, and the density and temperature can be determined from the mixture fraction via equations 5 and 4, respectively. Thus, for an open domain, the set of equations to be solved consists of the mixture fraction and momentum equations (equations 2 and 6), as well as an equation for the perturbation pressure. If the domain is not open, the density and temperature depend on time through both the mixture fraction and $p_o(t)$. This must be accounted for in a numerical scheme to conserve mass.

Isothermal Helium/Air Plume

The density ratio of air and helium, $\rho_{air}/\rho_{He} \approx 7$, is similar to the maximum ratio found in fires. Comparing results from helium plume simulations and

laboratory experiments, therefore, provides a test of the numerical approach used for the hydrodynamics in a buoyancy driven fire plume. The equation of state is

$$p_o(t) = \frac{\mathcal{R}\rho T}{W_{\text{air}}}\left(Y_{\text{He}}\left[\frac{W_{\text{air}}}{W_{\text{He}}} - 1\right] + 1\right) \qquad (7)$$

where Y_{He} is the helium mass fraction and W_{air} and W_{He} are the molecular weights of air and helium. If the domain is open, $p_o(t) = constant$. The motion of the gas is governed by the conservation equations of total mass, momentum (equation 6), and helium mass fraction. Adding the helium mass fraction equation multiplied by $(W_{\text{air}}/W_{\text{He}} - 1)$ to the continuity equation multiplied by $Y_{\text{He}}(W_{\text{air}}/W_{\text{He}} - 1)$ gives the equation for $p_o(t)$. Written in terms of ρ, this equation is

$$\frac{dp_o}{dt} + p_o\nabla\cdot\left(\frac{D_{12}}{\rho}\nabla\rho\right) = -p_o\nabla\cdot\underline{u} \qquad (8)$$

where D_{12} is the binary mass diffusivity; p_o satisfies this equation integrated over the volume. In the case of both an open or enclosed domain, equation 8 is a constraint on the divergence of the velocity field. With the divergence of the velocity from equation 8, the conservation equation for total mass is

$$\frac{\partial\rho}{\partial t} + \underline{u}\cdot\nabla\rho = \rho\left[\frac{1}{p_o}\frac{dp_o}{dt} + \nabla\cdot\left(\frac{D_{12}}{\rho}\nabla\rho\right)\right] \qquad (9)$$

Thus, in general, the set of equations to solve for a helium/air plume consists of the conservation equations for momentum and total mass (Equations 6 and 9) as well as equations for the perturbation and thermodynamic (Equation 8) pressures.

Numerical Model

The governing equations were nondimensionalized, written in two-dimensional cylindrical coordinates (i.e., axial symmetry is assumed), and solved with a finite difference technique on a staggered grid. Molecular values of the transport coefficients were used. Simulations of helium exiting from a pipe and a methanol pool fire were performed. The diameter of the pool (or pipe, in the helium case), D, the characteristic buoyant velocity, $U_b = \sqrt{Dg}$, and ambient air values of density, temperature, and so forth were used to nondimensionalize the equations. All spatial derivatives were approximated with second-order, accurate central differences with grid cells that were uniform in size in the axial direction and stretched in the radial direction. A second-order Runge-Kutta scheme was used for time stepping. The methodology is suitable for two or three spatial dimensions and any coordinate system for which a fast Poisson solver exists.

As was previously stated, an equation for the pressure perturbation, p, is required. Two methods were used, both of which resulted in a Poisson equation for p that was solved with a direct solver. The first method involved no physical assumptions. In the helium plume simulations, the pressure equation was obtained with a projection method similar to that employed by Davis et al. [7]. For the combustion case, a modification of the projection method was necessary for stability when high temperatures characteristic of pool fires were present (1800 K).

The second method used to obtain the perturbation pressure was based on physical assumptions regarding the generation of vorticity. There are three sources of vorticity: baroclinic generation due to the nonalignment of the pressure and density gradients, the effect of gravitational forces, and the contribution of spatial viscosity gradients. Equation 6 is simplified under the assumption that the contribution of the baroclinic torque to vorticity evolution is negligible. Under this assumption, the momentum conservation equation is

$$\frac{\partial\underline{u}}{\partial t} + \underline{\omega}\times\underline{u} + \nabla\left(\frac{1}{2}u^2\right) + \frac{1}{\rho_\infty}\nabla p - \left(1 - \frac{\rho_\infty}{\rho}\right)\underline{g} = \frac{1}{\rho}\nabla\cdot\underline{\underline{\sigma}} \qquad (10)$$

where $\underline{\omega}$ is the vorticity vector and $u^2 = \underline{u}\cdot\underline{u}$. Equation 10 does not allow baroclinic generation of vorticity and results from neglecting the term $(1/\rho - 1/\rho_\infty)\nabla p$ which is clearly negligible far from the reaction zone. The validity of this physical assumption, based on simulation results, is discussed later. Note that mass and energy conservation are not approximated. The equation for p was obtained by taking the divergence of equation 10. The divergence constraint of equation 8, for the helium problem, and its combustion analogue [5] were used in the determination of $\partial(\nabla\cdot u)/\partial t$. Unless otherwise stated, all simulated results refer to the first pressure solution method (i.e., no physical assumptions have been made).

Helium Plume Results

The experiments involved pure helium exiting into air from a 7.3 cm diameter circular pipe. Conditions were varied by changing the helium exit velocity, U_e, such that the range of Froude numbers covered was $0.0016 \le Fr \le 0.63$ $(Fr = U_e^2/Dg)$. The motion of the plume was expected to be controlled by buoyancy effects when Fr is small. Helium concentration measurements were made using laser-induced Rayleigh light scattering techniques [8].

Numerical simulations were begun by instantaneously rupturing an imaginary membrane covering the pipe opening. The helium exit velocity (top hat profile) was ramped up to match the experimental

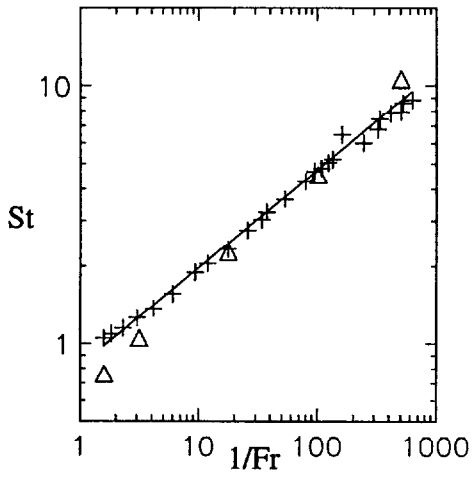

FIG. 1. Strouhal number ($St = fD/U_e$) of helium plume pulsations versus the inverse Froude number ($1/Fr = Dg/U_e^2$). Simulation results are denoted by Δ. Also shown are the experimental data of the current study (+) and the power law fit of the experimental data of Hamins et al. [1] ($St \propto (1/Fr^{0.38}$, ——).

velocity; there was no coflow. Results with a concentration-dependent viscosity coefficient (p. 641 of Williams [6]) were not appreciably different from those with a constant coefficient. Results reported here were obtained using a constant viscosity coefficient. Boundary conditions were such that the domain was either entirely enclosed or open (except for a floor). The method used for the open boundary conditions followed that of Mahalingham et al. [9]. In results reported here, the pipe orifice was located at floor level; raising the pipe orifice did not significantly change the results. Results were tested for grid independence by varying the spatial resolution. Time averages were computed over a range of plume pulsations (5 to 20) to ensure they were insensitive to the averaging time interval. The calculations presented here were on a grid with 192 cells in the radial direction and 768 cells in the axial, giving a maximum spatial resolution of 0.6 mm. This was a fairly expensive calculation with about 30 h of CPU time on an IBM/RISC 6000 workstation corresponding to 1 s of real time [48×10^{-6} cpu s/(cell · time step)]. A more realistic, three-dimensional simulation at the same temporal and spatial resolution would require a prohibitively larger amount of CPU time.

It is known experimentally [1,2] that the structure of the buoyant plume (with and without combustion) is governed by the periodic formation of toroidal vortices near the plume base. This is seen as time-trace oscillations in velocities, pressure, density, and so on near the plume base. The entrainment of air and, in the case of pool fires, flame length, combustion efficiency, and flame radiance are all influenced by the vortical structures and their frequency [1]. As a first check on the accuracy of the hydrodynamics, the frequency of the simulated plume pulsations (f) was checked against experimental values. Figure 1 is a plot of the Strouhal number, $St = fD/U_e$, versus the inverse of the Froude number. Results from the current experiment and the correlation of Hamins et al. [1] are in excellent agreement. The pulsation frequencies of the simulated plume can be seen to be in good agreement with the experiments over a large range of Froude numbers.

The baroclinic torque played a major role in the formation and frequency of the toroidal vortices at the base of the plume. This was clearly seen in the numerical simulations by turning off the baroclinic torque [i.e., using equation 10 in place of equation 6]. Without the baroclinic torque, the plume still oscillates due to gravitational effects, but with significantly higher frequencies. Animations of the simulation with and without the baroclinic torque ($Fr = 0.32$) can be viewed with a WWW browser in Mell et al. [10].

The major physical approximation in the simulation was that the plume evolves in an axisymmetric manner. Fluid motion across the centerline is not possible. This may increase the height at which the helium is "pinched off" by the rising toroidal vortex since air can cross the centerline only through molecular diffusion. Disagreement near the centerline between simulated and experimental values of the time-averaged mass fraction and axial velocity increased with height. This is seen in the radial profiles of the time-averaged helium mass fraction plotted in Fig. 2 for heights of $z/D = 0.1$, 1, 2.5 ($Fr = 0.6$). (Time-resolved comparisons of the simulation and experiment for $Fr = 0.32$ can be viewed with a WWW browser in Mell et al. [10]). The agreement between experiment and simulation clearly improves with radial distance from the centerline. Enforcing axial symmetry apparently resulted in significantly less mixing and greater buoyant acceleration in a volume near the centerline ($z/D < 0.2$) for heights greater than $z/D \approx 1$.

From the helium plume results presented above, it can be concluded that the numerical model used for the hydrodynamics captures much of the relevant physics in the lower region of the buoyant plume (where most of the combustion occurs) and is therefore suitable for use in a pool fire scenario.

Pool Fire Results

Experimental measurements of temperature in a 10-cm-diameter methanol pool fire were made. These measurements were not corrected for radiative heat loss from the thermocouple. This results in temperature measurements that are too low by an

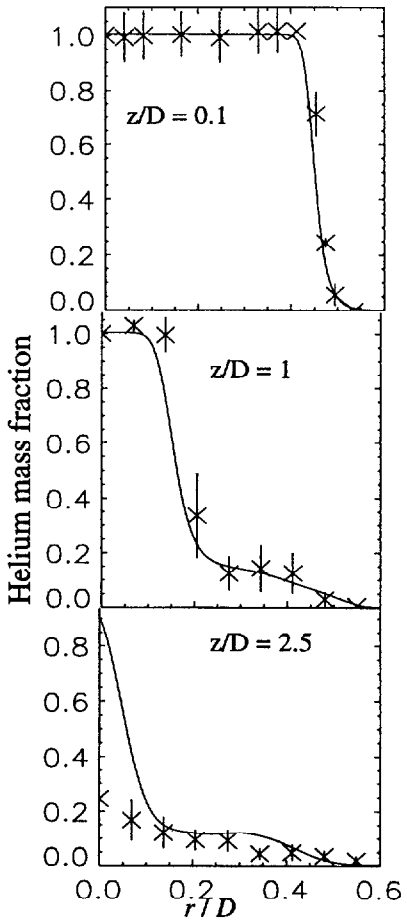

FIG. 2. Time-averaged radial profiles of the helium mass fraction at z/D = 0.1, 1, and 2.5. Simulation results are denoted by solid line. Experimental data (×) and rms variations (vertical lines) are also plotted; Fr = 0.6.

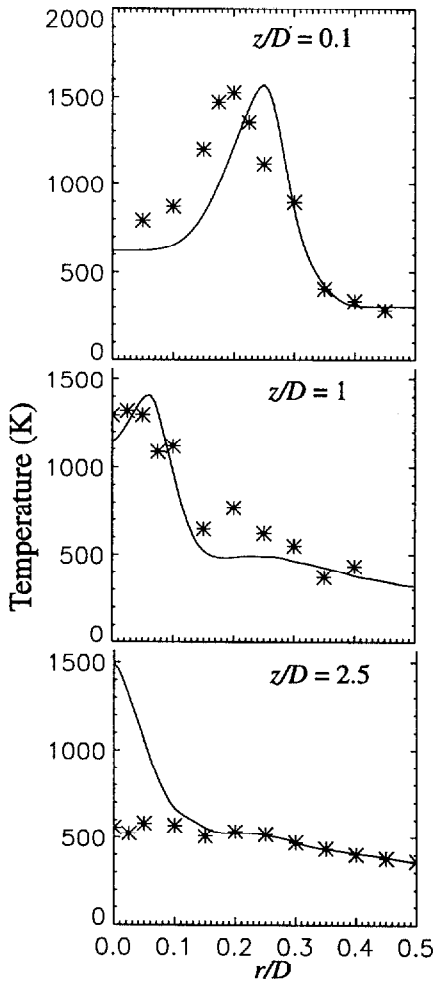

FIG. 3. Time-averaged radial profiles of temperature in the 10-cm methanol pool fire at z/D = 0.1, 1, and 2.5. Simulation results are denoted by solid line, experimental by asterisks; Fr = 0.0001.

amount that increases with temperature, equaling approximately 50 K at 1500 K [11].

Simulations of the 10-cm-diameter methanol pool fire used the mixture-fraction-based combustion model presented above. The flame sheet was located at Z_{st} = 0.133 with a temperature of 1800 K which corresponds to a radiative heat loss fraction of about 0.1; the pool temperature was 338 K (boiling temperature of methanol); and the axial velocity of the gaseous methanol at the pool surface was 1.1 cm/s which was consistent with experimentally measured mass burning rate. The Froude number was Fr = 0.0001; the Schmidt number was Sc = 0.7. The dynamic viscosity was temperature dependent but assumed to be independent of mixture composition. The average molecular weight was assumed to be constant (the effect of this was tested and found to be negligible for this fuel). Boundary conditions suitable for an enclosure were used which resulted in a 2% background pressure rise. Simulations on various domain sizes were run to confirm that confinement effects are not present. Time averages were computed over a range of pool flickering cycles (5–20) to ensure they were insensitive to the averaging time interval. The calculations presented here were performed on a grid with 192 cells in the radial direction and 640 in the axial, giving a maximum spatial resolution of 0.78 mm. Roughly 60 h of CPU time on a IBM/RISC 6000 workstation were required for 1 s of real time [80 × 10^{-6} cpu s/(cell · time step)]. Simulations made with a higher spatial resolution (0.5 mm) produced nearly identical time averages.

Temperature time traces at the base of the plume

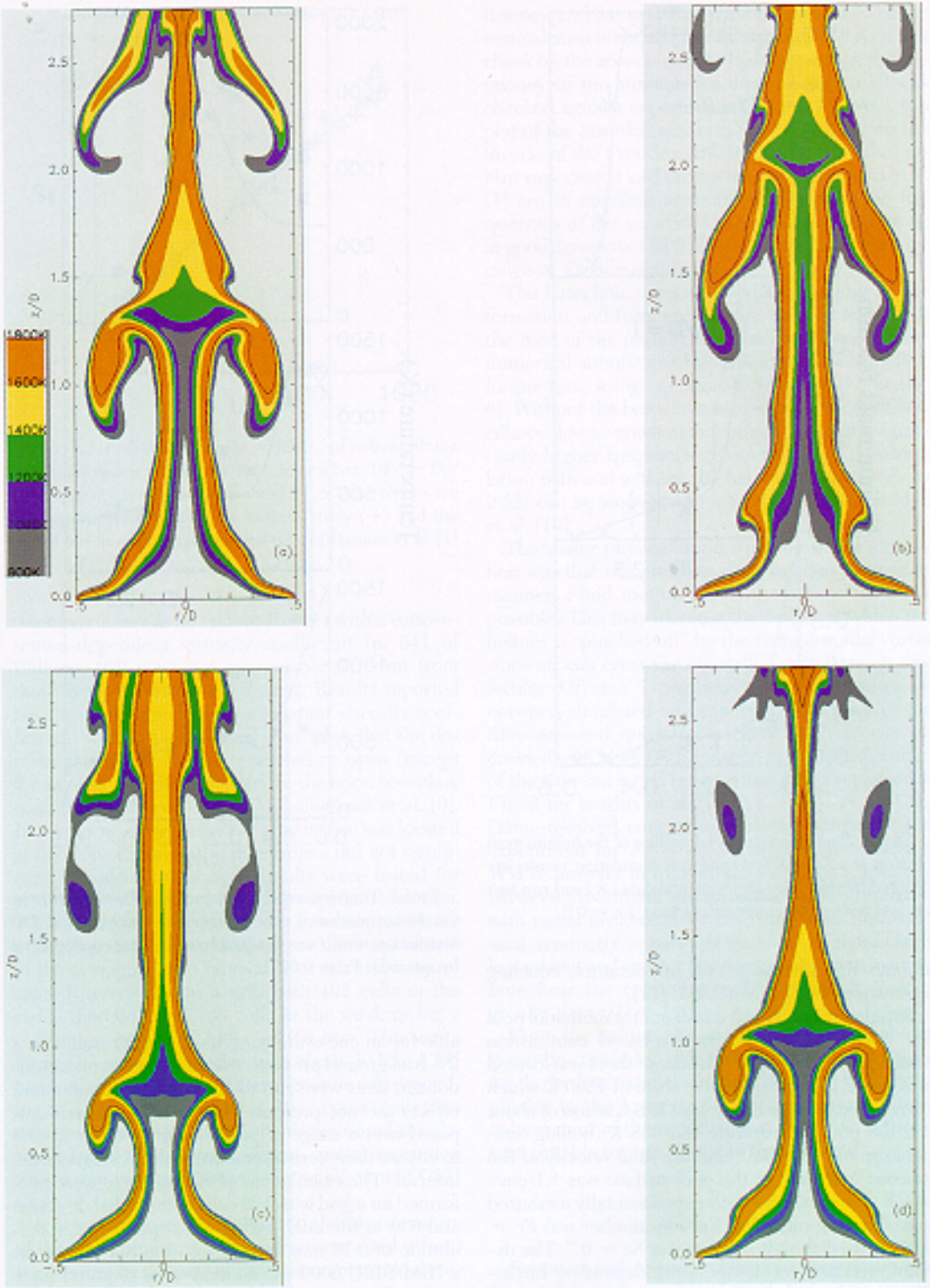

FIG. 4. Contours of temperature field in the 10-cm methanol pool fire at four successive times over one cycle of the temperature time trace at the base of the pool; $Fr = 0.0001$. Time increases from (a) to (d). The flame sheet is located at $T = 1800$ K which is contoured by a red line.

oscillated periodically with frequencies of 5.6 Hz and 7.0 Hz in the experiment and simulation, respectively. Pagni [12] provides a compilation of a number of studies; frequencies for 10-cm pool fires of a variety of fuels range from about 4 Hz to 10 Hz. Thus, the flicker frequency of the simulated plume was within the measured range. Simulations with and without the baroclinic torque were also compared. The baroclinic torque had even more influence on the development of the toroidal vortices than for the helium plume. Without the baroclinic torque, the fire plume oscillated at higher frequencies and the onset of oscillations was significantly delayed.

Time-averaged radial profiles of the temperature from the experiment and simulation are shown on Fig. 3. As in the case of the helium plume for heights larger than $z/D \approx 1$, the simulated time averages increasingly deviate from their experimental values near the centerline ($r/D < 0.2$). The possible causes of this deviation are the assumption of axial symmetry and approximations inherent in the combustion model. Based on the helium plume results, errors due to the axial-symmetry approximation are not expected below $z/D \approx 1$. Thus, the simplifications implied by the mixture-fraction-based combustion model are the probable cause of the disagreement at $z/D = 0.1$ in Fig. 3.

Figure 4 shows plots of the instantaneous temperature field over one cycle in the temperature time trace at the plume's base. Time increases from Fig. 4a to 4d, with the plots separated in time by approximately 1/20 s. The flame sheet location $T = 1800$ K is shown as a red contour line. As is expected for a pool fire of this size, the flow appears to be laminar. In Fig. 4a, a vortex is forming at the base of the plume and previously formed vortices are present at $z/D \approx 1.1$, 2.3. The spatial separation of the vortices increases with time due to buoyant acceleration. By noting the position of the flame sheet, the process of flame flickering can be seen. Initially, the flame tip rises due to both the vorticity-induced flow field and buoyancy. The flame tip then accelerates upward due to buoyancy and has detached from the lower flame in Fig. 4d. In an approximate manner, this behavior was repeatable. From video recordings, the flame tip "pinches off" at comparatively lower heights in the experimental pool fire. This is consistent with the larger, time-averaged temperatures in the simulation near the centerline in Fig. 3.

Conclusions

A numerical simulation of a 10 cm methanol pool fire was performed. The hydrodynamics were simplified by assuming the motion to be axially symmetric. The numerical approach used for the hydrodynamics was tested by simulating a number of experimental helium plumes of similar size to the fire plume. Both the instantaneous and time-averaged behavior of the experimental helium plume was well reproduced by the simulation for heights up to $z/D \approx 1$. Above this height, three-dimensional effects not accounted for in the simulations were present. Comparisons of numerical results with a 10-cm-diameter pool fire experiment indicate that the instantaneous and time-averaged behavior of the large-scale plume structure were reasonably well calculated. As in the helium case, with increasing height, the assumption of axial symmetry broke down, causing prediction errors in a volume surrounding the centerline ($r/D < 0.2$). It is clear that obtaining the full plume structure for $z/D > \mathcal{O}(1)$ requires a three-dimensional analysis. The computational cost of these axially symmetric simulations is sufficiently large to prohibit three-dimensional calculations with the same methodology (i.e., direct numerical simulations). To this end, the current combustion model is being incorporated into the thermal element component of the large eddy simulation method of Baum et al. [4] for three-dimensional simulations of large fires.

Acknowledgments

The authors gratefully acknowledge the following for helpful discussions and for making their experimental data available: Drs. Art Johnson and William Pitts (helium plume), and Mr. Nikolai Gorchkov and Dr. Anthony Hamins (methanol pool fire).

REFERENCES

1. Hamins A., Yang, J. C. and Kashiwagi, T., *Twenty-Fourth Symposium (International) on Combustion,* The Combustion Institute, Pittsburgh, 1992, pp. 1695–1702.
2. Cetegen, B. M. and T. A. Ahmed, *Combust. Flame* 93:157–184 (1993).
3. Rehm, R. G. and H. R. Baum, *J. Res. NBS* 83:297–308 (1978).
4. Baum, H. R., Ezekoye, O. A., McGrattan, K. B., and Rehm, R. G., *J. Theor. Comput. Fluid Dyn.* 6:125–139 (1994).
5. Baum, H. R., Rehm, R. G., and Gore, J. P., *Twenty-Third Symposium (International) on Combustion,* The Combustion Institute, Pittsburgh, 1990, pp. 715–722.
6. Williams, F. A., *Combustion Theory,* 2nd ed., Benjamin Cummings, Menlo Park, CA, 1985, pp. 73–76.
7. Davis, R. W., Moore, E. D., Chen, L. -D., Roquemore, W. M., Vilimpos, V., and Goss, L. P., *Theor. Comput. Fluid Dyn.* 6:113–123 (1994).

8. Pitts, E. M. and Kashiwagi, T., *J. Fluid Mech.* 141:391–429 (1984).
9. Mahalingham, S., Cantwell, B. J., and Ferziger, J. H., *Phys. Fluids A* 2:720–728 (1990).
10. Mell, W. E., McGrattan, K. B., Baum, H. R., Johnson, A. W., and Pitts, W. M., Fall 1995 Western States Section meeting/Combustion Institute, Stanford, CA, Paper No. 95F-221, http://odie.seas.ucla.edu/WSS/papers/f95/95F221.html.
11. Smyth, K. C., Miller, J. H., Dorfman, R. C., Mallard, W. G., and Santoro, R. J., *Combust. Flame* 62:157–181 (1985).
12. Pagni, P. J., in ASME Paper No. 89-WA/FE-5 Trefethen, L. M. and Panton, R. L., 1989, p. 26.

COMMENTS

Ahmed F. Choniem, Massachusetts Institute of Technology, USA. What was the value of the Reynolds number for these simulations and did you compare the results for different Reynolds numbers?

Do you think that the Reynolds number could have an effect on the delayed pinching in the axisymmetric model?

Author's Reply. Since molecular values of the transport coefficients were used the Reynolds number for the 10 cm pool based on the buoyant velocity ($U_b = \sqrt{[gD]}$), pool diameter (D), and ambient air viscosity is Re $\approx$ 6000; if the axial velocity at the pool surface is used Re $\approx$ 70. The corresponding Reynolds numbers for the helium plume are Re $\approx$ 3000 and for the different exit velocities Re $\approx$ 3000, 2000, 900, 360, 170 (U_e = 0.67, 0.48, 0.2, 0.08, 0.038 m/s). Thus, only one Reynolds number was considered for the pool fire.

Pinching in the simulated helium plume was delayed in all Re cases; no significant Re effects existed. Comparison of a video recording of the experimental helium plume (case Re $\approx U_eD/\nu$ = 2000) to an animation of the axially symmetric simulation clearly showed that, except at small heights, the experimental plume is not axisymmetric (this can be viewed with a web browser [10]). This is also seen in plots of both the time averaged helium mass fraction (Fig. 2; Re = 3000) and temperature (Fig. 3) and is the most likely cause of the delayed pinching in the simulations.

•

K. Kailasanath, Naval Research Laboratory, USA. For the methanol fire simulations, could you comment on the boundary conditions at the liquid interface? Was the fuel evaporation unsteady and did you take into account effects such as the radiation to the surface from the puffing fire?

Author's Reply. Steady, uniform evaporation of methanol across the pool surface was assumed. The boiling temperature of methanol (338 K) defined the density. Zero radial velocity and an axial velocity (1.1 cm/s) consistent with experimentally measured mass burning flux (13 gm/m^{2}s) were used. These quantities define the axial gradient of the perturbation pressure across the pool surface. Radiative heat transfer was not part of the calculation. Instead, all locations in the flame were assumed to have lost a fixed amount of chemical heat release due to radiation to the surroundings. Heat transfer to the pool surface through radiation (along with convection and conduction) causes fuel boiling which is accounted for in the boundary condition.

•

F. S. Marra, DETEC—University of Naples "Federico II," Italy. You explained that a projection method was adopted in deriving the equation for the pressure term appearing in the momentum balance equation. This in my opinion implies that any disturbance (also numerical) is immediately propagated in the whole computational domain. This suggest that the boundary conditions, difficult to specify especially on the outlet section, can affect the whole computation.

Did you find it necessary to use a special treatment of the boundary conditions, mainly with respect to the influence on the natural characteristic frequency of the phenomenon?

Author's Reply. Due to the elliptic nature of the conservation equations it is important that the boundary conditions are accurately specified. Your statement is correct; outlet boundary conditions are much more difficult to implement than those for a wall. As mentioned in the text, boundary conditions suitable for both an open (except for a floor) and a completely enclosed domain were used for the helium plume. The puffing frequency of the helium plume was not found to depend on the type of boundary condition used. In the pool fire simulation the domain was completely enclosed. Attempts to use open boundary conditions analogous to those in the helium plume simulation were unsuccessful. This was due to the presence of a slowly rising vortex passing through the upper boundary (which was not present in the helium plume case). The domain size was varied to ensure that there were no confinement effects on the behavior of the plume (including the flicker frequency).